Three-dimensional discrete element analysis of triaxial tests on crushable pumice sand

Analyse par d'éléments discrets tridimensionnels d'essais triaxiaux sur du sable ponce écrasable

Rolando P. Orense & Sayed Hessam Bahmani
Dept. of Civil & Environmental Engineering, University of Auckland, Auckland, New Zealand

ABSTRACT: From an engineering viewpoint, pumice sand particles are problematic because of their crushability and compressibility. While laboratory and in-situ tests can be implemented to characterise their behaviour, these tests are generally time-consuming and expensive. In this paper, the monotonic shear behaviour of crushable pumice sand specimens is examined using the Discrete Element Method (DEM). Each pumice particle is modelled as a sphere that, when the maximum contact force reaches the limit condition, will break and split into 14-ball inscribed tangent spheres. Initially, the results of laboratory single particle crushing tests are used to represent the breakage characteristics as a function of particle size. Next, using the open-source code YADE, 3D model specimens in loose and medium dense states are prepared and isotropically consolidated at prescribed levels of confining pressure. The numerical specimens are then subjected to monotonic loading under both drained and undrained conditions. The results showed that the DEM model could replicate the laboratory-obtained experimental results, offering explanations on the effect of particle crushing on the stress-strain relations. The microscale observations also provide better insights into the evolution of force-chains within the specimens, resulting in a clearer understanding of pumice sand behaviour during shearing.

RÉSUMÉ : D'un point de vue technique, les particules de sable ponce sont problématiques en raison de leur aptitude à l'écrasement et de leur compressibilité. Si des tests essai en laboratoire et in situ peuvent être mis en œuvre pour caractériser leur comportement, ces essai sont généralement longs et coûteux. Dans cet article, le comportement en cisaillement monotone des échantillons de sable ponce écrasable est examiné à l'aide de la méthode des éléments discrets (DEM). Chaque particule de pierre ponce est modélisée comme une sphère qui, lorsque la force de contact maximale atteint la condition limite, se brise et se divise en 14 sphères tangentes inscrites. Dans un premier temps, les résultats des essais de broyage de particules uniques en laboratoire sont utilisés pour représenter les caractéristiques de rupture en fonction de la taille des particules. Ensuite, en utilisant le code open source YADE, des échantillons 3D dans des états lâches et moyennement denses sont préparés et consolidés de manière isotrope à des niveaux prescrits de pression de confinement. Les échantillons numériques sont ensuite soumis à un chargement monotone dans des conditions à la fois drainées et non drainées. Les résultats ont montré que le modèle DEM est capable de reproduire les résultats expérimentaux obtenus en laboratoire, offrant des explications sur l'effet de l'écrasement des particules sur les relations contrainte-déformation. Les observations à l'échelle microscopique fournissent également de meilleures informations sur l'évolution des chaînes de force dans les spécimens, ce qui permet une meilleure compréhension du comportement du sable ponce pendant le cisaillement.

KEYWORDS: crushable soils; pumice sand; distinct element model; triaxial test.

1 INTRODUCTION

As a result of volcanic eruptions in the Taupo Volcanic Zone (TVZ), pumiceous materials are widely deposited in the central part of the North Island in New Zealand. The concentration of the pumiceous materials in the river valleys and flood plains in the region means that they are frequently encountered in many engineering projects. Therefore, the evaluation of their properties is a matter of considerable geotechnical interest. These materials contain pumice sands, which are highly crushable, compressible and lightweight due to the vesicular nature of the particles. These characteristics make them problematic for practising engineers since many of the analytical frameworks and correlations which are currently used have been developed for quartz-type (hard-grained) sands.

The Geomechanics Group of the University of Auckland has been investigating the geotechnical properties of pumice sands by performing calibration chamber tests and various laboratory element tests (e.g. Wesley et al., 1999; Pender et al., 2006; Orense et al., 2012; Kikkawa et al., 2013). While the test results have provided insights on the geotechnical properties of crushable pumice sands, more tests are necessary to characterise their behaviour. However, such tests are generally time-consuming and expensive to perform.

To address the above challenges, the use of the discrete element method (DEM) as an alternative/supplementary tool is explored. DEM can integrate the information obtained from observational analyses and laboratory experiments while examining the behaviour of particulate materials. As a result, it allows for both macroscale (specimen level) and microscale (particle level) observations, thereby enabling the investigation of specific parameters that are either difficult or very expensive to be directly observed in standard laboratory tests or in-situ tests (Cundall, 1988). Various researchers have conducted many DEM studies to examine the behaviour of granular materials during laboratory tests (e.g., Belheine et al., 2009; Cil & Alshibli, 2014; Gong et al., 2012; O'Sullivan, 2011).

In this paper, three-dimensional DEM models are formulated to investigate the monotonic drained and undrained response during triaxial tests of crushable pumice sand specimens, whose particles can be crushed by pressing with a fingernail. For this purpose, the open-source software YADE is used. This software allows for a high degree of customisation, such as the development of new contact models and new particle geometries, through writing computational codes with a flexible object model (Šmilauer et al., 2010). Actual experimental results on pumice sand specimens were used to calibrate and validate the models. The study enables the development of a qualitative understanding of the response of crushable soil from a micro-mechanics perspective.

2 PARTICLE CRUSHING

2.1 *Single particle crushing tests*

To examine how the particle strength varies with the size of the particle, single particle crushing tests were conducted on pumice particles with nominal sizes ranging from 1 – 8 mm. Approximately 30 particles were tested for each nominal size. The results obtained were consistent with those reported by Orense et al. (2013), which showed that the particle crushing strength, σ_c, decreases with increasing particle size, d. The results are then expressed in terms of the probability of the particle surviving the crushing, P_s, as a function of σ_c (see Figure 1). Next, the statistical model originally formulated by Weibull (1951) and extended by McDowell & Bolton (1998) was used to represent the probability of survival, P_s, i.e.

$$P_s(d) = exp\left[-\left(\frac{d}{d_0}\right)^3\left(\frac{\sigma_c}{\sigma_0}\right)^m\right] \quad (1)$$

where σ_0 is the crushing strength at which 37% of the tested particles survive and is approximately equal to the mean tensile strength of particles of size d_0. In Eqn (1), m is the Weibull modulus, which can be described as a shape parameter for the Weibull distribution model, i.e., a high value indicates little strength variation from particle to particle. The results of the analysis show that for pumice sand, m=1.17, much lower than those reported in the literature for various granular materials, indicating that physical flaws (such as surface and internal voids) within the particles are clustered inconsistently, and the measured strength is broadly distributed.

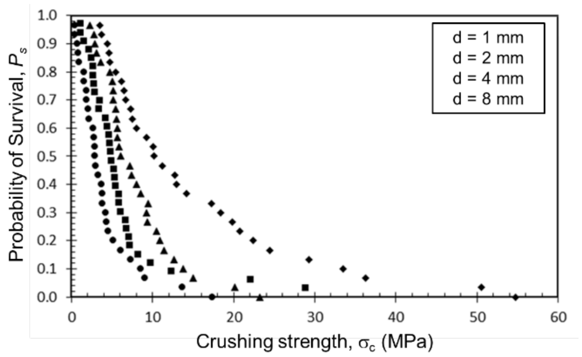

Figure 1. Weibull distribution of pumice particle strengths, showing the variation of probability of survival with crushing strength.

2.2 *Particle crushing criteria*

In the DEM, the failure criteria adopted are based on the approach of Russell et al. (2009), considering the Von Mises criterion. Here, a particle subject to several external force points may crush when the applied force, F, exceeds the following limit conditions:

$$F \geq \sigma_{lim} \cdot A_F \quad (2)$$

where σ_{lim} is the particle strength limit, and A_F is the contact area. The particle strength limit is assumed to be normally distributed for a particular particle size d, whose mean strength factor, $\bar{\sigma}_{lim}$, is given by:

$$\bar{\sigma}_{lim} = \sigma_{lim0} \cdot f(Var) \cdot \left(\frac{d}{d0}\right)^{-3/m} \quad (3)$$

where σ_{lim0} is the mean limit strength of a particle with diameter d_0, and $f(Var)$ represents the influence of the particle strength variation. The following expression can be obtained by using the linear contact theory (Ciantia et al., 2019):

$$F \leq \left\{\sigma_{lim0} \cdot f(Var) \cdot \left(\frac{d}{d0}\right)^{-\frac{3}{m}} \pi\left[\frac{3}{4}\frac{\left(\frac{1-\nu_1^2}{E_1}+\frac{1-\nu_2^2}{E_2}\right)}{\left(\frac{1}{r_1}+\frac{1}{r_2}\right)}\right]^{2/3}\right\}^3 \quad (4)$$

where r_1 and r_2 are the radii of the contacting spheres, and E_i and ν_i are the Young's moduli and Poisson's ratios, respectively. Note that this breakage criterion does not only relate strictly to maximum force on the particle but also to the characteristics of the contacting particles. Once the limit condition is reached, a spherical particle will split into smaller, inscribed tangent spheres. Ciantia et al. (2015) detailed the procedure involved and reported that the 14-ball splitting configuration, shown in Figure 2, is accurate enough to simulate the macroscopic behaviour. After crushing, exemplified by the splitting of the smaller spheres, the daughter fragments assume the velocity and material parameters of the mother particle, except for the intrinsic strength (σ_{lim0}), which is randomly distributed among the particles.

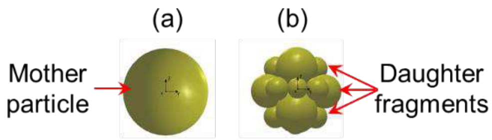

Figure 2. Modelling particle crushing in DEM: (a) original particle; (b) particle splitting configuration.

3 DEM MODELING

3.1 *DEM specimen preparation and testing*

Prismatic sand specimens (10 mm ×10 mm × 20 mm), each comprising 10,000 spherical particles, were prepared at the pre-defined relative densities, as shown in Figure 3. While the specimens have particle size distributions that were the same as those used in the actual experiments, the figure represents the particle sizes in terms of different colours, i.e., blue represents the smaller sizes while red shows the bigger sizes.

The specimens were initially created using the radius expansion method (REM), where the particles were randomly placed within the target specimen volume without any locked-in force or overlap (Ciantia et al., 2015). The particles are then slowly expanded until the desired radii are reached while keeping the consolidation pressure on boundaries constant. During the expansion process, the contact force evolution between two particles causes the particles to move and rotate so that, to maintain equilibrium for a specimen at a target state, the boundary positions are allowed to change accordingly. Once the desired radii have been achieved, the inter-particle friction coefficient is reset to the expected value. The detail of the input parameters is found in Table 1.

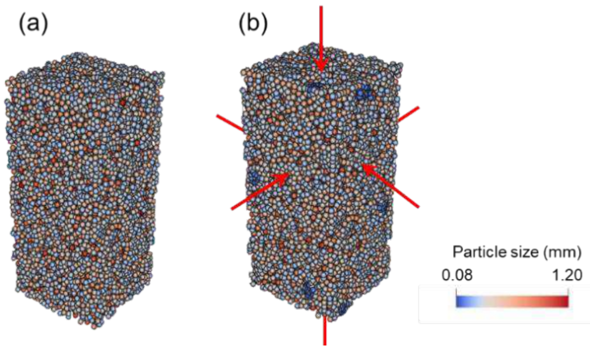

Figure 3. DEM model of triaxial specimen: (a) before application of REM; (b) during consolidation.

While various types of contact models are available in YADE, this study made use of the linear contact model, which obeys the Coulomb friction law. Here, a linear relationship is assumed between the normal force and the allowable shear force. The model describes the constitutive behaviour in normal and tangential directions between particles at their contact interface by adopting linear springs with normal and shear stiffnesses (Cundall & Strack, 1979). A rolling resistance model, based on the formulation of Iwashita & Oda (1998), was incorporated to simulate the surface roughness of pumice particles.

Table 1. DEM input parameters

Parameters	Value	Unit
Coefficient of friction, μ	0.7	-
Young's modulus, E	30.1	MPa
Poisson's ratio, ν	0.25	-
Coefficient of rolling stiffness, β	0.125	-
Coefficient of rolling strength, η	0.10	-

In the monotonic drained test, the bottom boundary of the specimen is fixed, whereas the top boundary undergoes vertical motion at a rate of 0.1 mm/sec. On the other hand, the constant volume method is adopted in the monotonic undrained test; here, the fluid phase is neglected, the specimen volume remains constant during the loading process, and the inter-particle contact forces are monitored. A periodic boundary is assumed for the lateral sides of the specimen, and vertical loading is applied at the top with a strain rate of 0.1/sec while maintaining constant volume condition.

3.2 *DEM simulation of monotonic drained tests*

The drained monotonic behaviour of pumice sand specimens, as reported by Kikkawa et al. (2013) and Pender et al. (2006), are simulated using DEM to get better insights into the behaviour of crushable pumice sands. Figure 4 shows the comparison between the experiments and simulations in terms of the variation of the deviatoric stress and volumetric strain with respect to the axial strain for loose pumice specimen (relative density, Dr=25%) under two levels of confining pressure (σ'_0=100 and 400 kPa). Other values of σ'_0 were simulated as well, as shown in the figure.

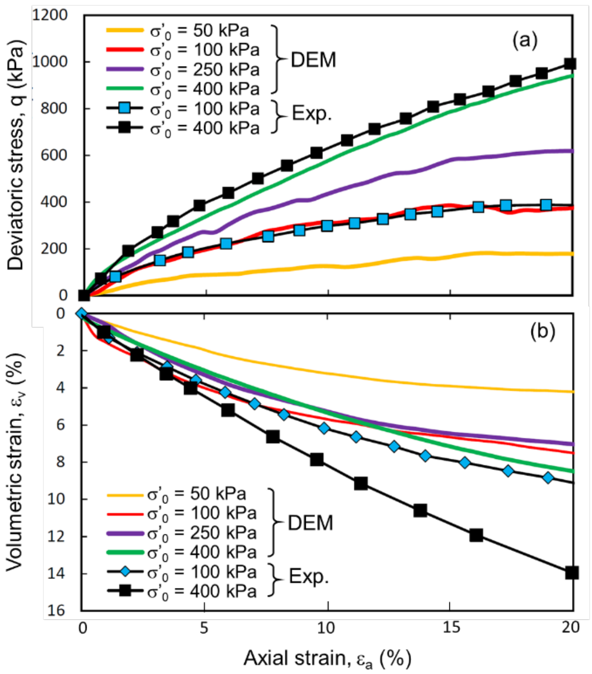

Figure 4. Comparison between the results of experimental and DEM simulation for loose pumice sand specimen: (a) deviatoric stress-axial strain; (b) volumetric strain-axial strain.

It is observed that, while the stress-strain response is captured very well for both levels of confining pressures, the DEM simulation underestimates the volumetric change, especially under higher confining pressure. This can be attributed to the higher compressibility of the pumice sands, which was not fully captured by the DEM model.

The evolution of the contact force with strain is illustrated in Figure 5. In the figures, the contact forces, expressed in N, join the centres of the particles and the line colour is proportional to the magnitude of the force (forces exceeding the average values are illustrated in orange, those with high magnitudes are in red, and low force values are in blue). With increasing axial strain, the magnitude of the normal contact forces increases (as indicated by the change in colour from blue to red), with a higher level of the increase concentrated at the centre of the specimen, an indication that particle crushing is occurring more at this zone. This behaviour is less evident at lower confining pressure because of the lesser number of crushing events and rearrangement between particles being more dominant.

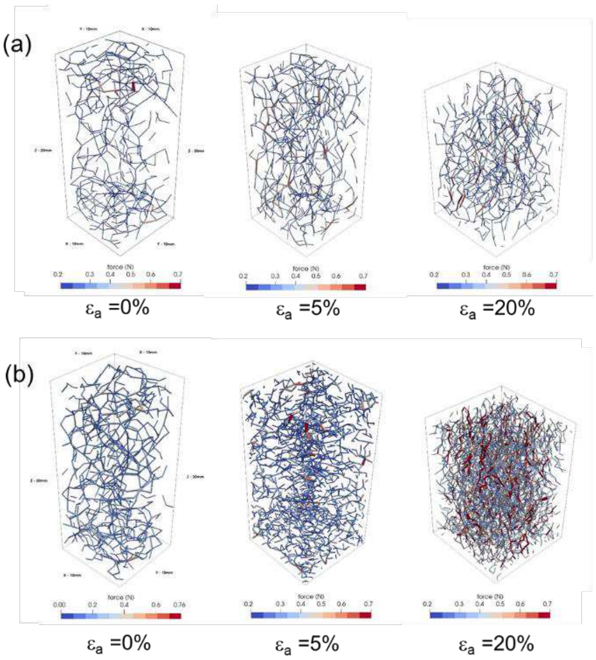

Figure 5. Contact force distribution within the specimen at various stages of the tests under confining pressures of: (a) 100 kPa; (b) 400 kPa.

In addition to the contact forces network, the DEM results also provided other micro-level details, such as the evolution of particle crushing and mechanical coordination number. Although not shown here, mechanical coordination number (indicating the average number of contacts a particle has) increases with axial strain as the particles are crushed during shearing, leading to the formation of new contacts. This behaviour is more evident under higher confining pressure.

3.3 *DEM simulation of monotonic undrained tests*

Next, the undrained monotonic test results reported by Orense et al. (2012) are simulated. The comparison between the experiments and the simulation is shown in Figure 6 for the loose specimen (*Dr*=29%) under σ'_0=50-400 kPa. It appears that, based on the results, while DEM can capture the undrained response at low confining pressure levels, specimens under higher confining pressures tend to be less stiff and less contractive; as in the drained case, this may be due to the higher compressibility of pumice sands which was not fully captured by the DEM model.

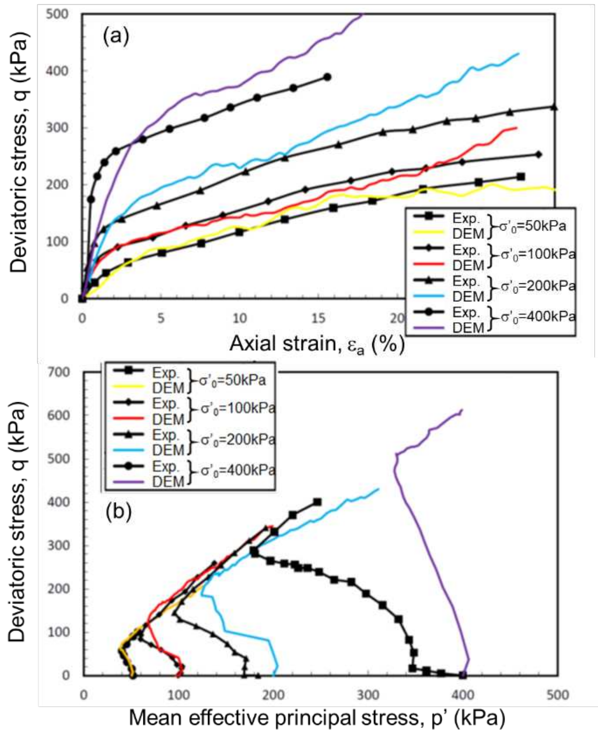

Figure 6. Comparison between the results of experimental and DEM simulation for loose pumice sand specimens under different σ'_0: (a) deviatoric stress-axial strain; (b) effective stress paths.

Figure 7 illustrates the evolution of the contact forces at various stages of the tests under σ'_0=100 kPa. It can be observed that the contact forces are more evenly distributed with the adoption of periodic boundary condition, which induced less contact force between the particles and the side boundary. At ε_a=10%, the contact forces appeared to increase even with the increase in pore water pressure; however, at ε_a=20%, the network becomes more reddish, indicating an increase in contact forces possibly due to stronger interlocking between the particles as a result of particle crushing. Focusing on the micro-level response, the coordination number is observed to decrease initially as a result of particle rearrangement and the development of pore water pressure. Then, with continuous shearing, it increases as the particle crushing and grain-to-grain interlocking continue.

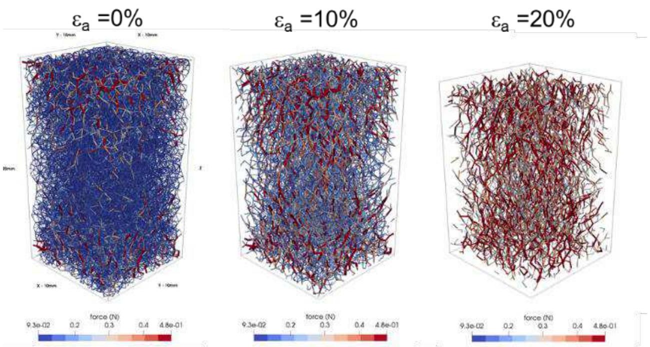

Figure 7. Contact force distribution within the loose specimen at various stages of the tests under a confining pressure of 100 kPa.

4 CONCLUSIONS

In this paper, the discrete element method (DEM) was used to simulate the drained and undrained monotonic test results of specimens consisting of crushable pumice sands. The results of the simulations demonstrated that the developed DEM model, which incorporated the strong dependency of crushing strength on the particle size into the particle crushing criteria, and complemented by the use of linear contact model that considered rolling resistance, can generally capture the macro-behaviour of pumice sand in monotonic triaxial condition. Moreover, the DEM model provided opportunities to look at the micro-level response, such as the evolution of contact forces, the number of crushing events and particle contacts, during the testing process.

5 ACKNOWLEDGEMENT

This research was conducted by the first author as part of his PhD research at the University of Auckland. As part of this research, the New Zealand eScience Infrastructure (NeSI) high-performance computing facilities are also acknowledged. New Zealand's national facilities are provided by NeSI and funded jointly by NeSI's collaborator institutions and through the Ministry of Business, Innovation & Employment's Research Infrastructure programme (https://www.nesi.org.nz).

6 REFERENCES

Belheine, N., Plassiard, J.-P., Donzé, F.-V., Darve, F., & Seridi, A. 2009. Numerical simulation of drained triaxial test using 3D discrete element modeling. *Computers and Geotechnics*, 36(1-2), 320-331.

Ciantia, M., Arroyo, M., Calvetti, F., & Gens, A. 2015. An approach to enhance efficiency of DEM modelling of soils with crushable grains. *Géotechnique*, 65(2), 91-110.

Ciantia, M. O., Arroyo, M., O'Sullivan, C., & Gens, A. 2019. Micromechanical inspection of incremental behaviour of crushable soils. *Acta Geotechnica*, 14(5), 1337-1356.

Cil, M. B., & Alshibli, K. A. 2014. 3D analysis of kinematic behavior of granular materials in triaxial testing using DEM with flexible membrane boundary. *Acta Geotechnica*, 9(2), 287-298.

Cundall, P. A. 1988. Formulation of a three-dimensional distinct element model—Part I. A scheme to detect and represent contacts in a system composed of many polyhedral blocks. *Int. Jour. Rock Mech and Mining Sciences & Geomechanics Abstracts*, 25(3), 107-116.

Gong, G., Thornton, C., & Chan, A. H. 2012. DEM simulations of undrained triaxial behavior of granular material. *Journal of Engineering Mechanics*, 138(6), 560-566.

Iwashita, K., & Oda, M. 1998. Rolling resistance at contacts in simulation of shear band development by DEM. *Journal of Engineering Mechanics*, 124(3), 285-292.

Kikkawa, N., Pender, M., & Orense, R. 2013. Comparison of the geotechnical properties of pumice sand from Japan and New Zealand. *Proc., 18th Int. Conf. on Soil Mech & Geotech Eng.*, Paris.

McDowell, G., & Bolton, M. 1998. On the micromechanics of crushable aggregates. *Géotechnique*, 48(5), 667-679.

Orense, R., Pender, M., & O'Sullivan, A. 2012. Liquefaction characteristics of pumice sands. *EQC Project Report 10/589*, Earthquake Commission.

Orense, R., Pender, M. J., Hyodo, M., & Nakata, Y. 2013. Micro-mechanical properties of crushable pumice sands. *Geotechnique Letters*, 3, 67-71.

O'Sullivan, C. 2011. *Particulate Discrete Element Modelling: a Geomechanics Perspective*. CRC Press.

Pender, M., Wesley, L., Larkin, T., & Pranjoto, S. 2006. Geotechnical properties of a pumice sand. *Soils and Foundations*, 46(1), 69-81.

Russell, A. R., Wood, D. M., & Kikumoto, M. 2009. Crushing of particles in idealised granular assemblies. *Journal of the Mechanics and Physics of Solids*, 57(8), 1293-1313.

Šmilauer, V., Catalano, E., Chareyre, B., Dorofeenko, S., Duriez, J., Gladky, A., Kozicki, J., Modenese, C., Scholtès, L., & Sibille, L. 2010. Yade reference documentation. *Yade Documentation*, 474.

Weibull, W. 1951. A statistical distribution function of wide applicability. *Journal of Applied Mechanics*, 18(3), 293-297.

Wesley, L., Meyer, V., Pranjoto, S., Pender, M., Larkin, T., & Duske, G. 1999. Engineering properties of a pumice sand. *Proc. 8th Australia New Zealand Conference on Geomechanics*, 2, 901-908.